

SMEFT projections of neutral-current PVDIS asymmetries at the EIC

Kağan Şimşek

Northwestern
University

in collaboration with

Radja Boughezal, Alexander Emmert, Tyler Kutz, Sonny Mantry,
Michael Nycz, Frank Petriello, Daniel Wiegand, and Xiaochao Zheng

reference: [PRD 106 \(2022\) 016006 \[2204.07557\]](#)

EIC Early Career Workshop 2022
CFNS Stony Brook University

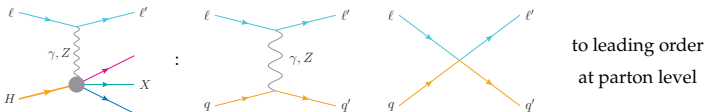
July 24-25, 2022

- We study NC DIS cross-section asymmetries at EIC.
- BSM effects are parametrized in SMEFT framework.
- Higher-dimensional operators are built of existing SM particles with Wilson coefficients as effective couplings at UV scale Λ :

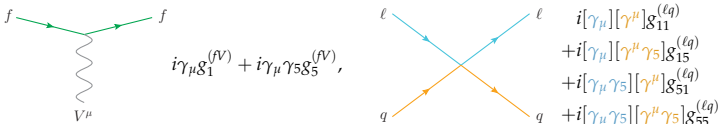
$$\mathcal{L}_{\text{SMEFT}} = \mathcal{L}_{\text{SM}} + \sum_{n>4} \frac{1}{\Lambda^{n-4}} \sum_k C_k^{(n)} O_k^{(n)}$$

- All new physics is assumed to be heavier than all SM states and accessible collider energy.
- We focus on semi-leptonic 4-fermion $O_k^{(n)}$ at $n = 6$.
- We find that the EIC can
 - probe complementarily and competitively to LHC DY
 - resolve blind spots observed in LHC NC DY data fits

We study the NC DIS in the process $\ell + H \rightarrow \ell' + X$, where $\ell = e^-, e^+$ and $H = p, D$:



We parameterize the vertex factors in terms of vector and axial couplings:



We don't consider Yukawa or dipole interactions because they are suppressed by fermion masses, which we assume to vanish.

SMEFT operators shift the usual vector and axial SM couplings in a gauge-invariant way: e.g.

$$g_1^{(fZ)} = g_V^f + \mathcal{O}(C_k), \quad g_5^{(fZ)} = g_A^f + \mathcal{O}(C_k)$$

Operators that contribute to the ffV and $\ell\ell qq$ vertices at dimension 6 are (Grzadkowski *et al.* [[1008.4884](#)]):

ffV	$\ell\ell qq$
$O_{\phi\ell}^{(1)} = (\varphi^\dagger i \overleftrightarrow{D}_\mu \varphi)(\bar{\ell}\gamma^\mu\ell)$	$O_{\ell q}^{(1)} = (\bar{\ell}\gamma_\mu\ell)(\bar{q}\gamma^\mu q)$
$O_{\phi\ell}^{(3)} = (\varphi^\dagger i \overleftrightarrow{D}_\mu \tau^I \varphi)(\bar{\ell}\gamma^\mu\tau^I\ell)$	$O_{\ell q}^{(3)} = (\bar{\ell}\gamma_\mu\tau^I\ell)(\bar{q}\gamma^\mu\tau^I q)$
$O_{\phi e} = (\varphi^\dagger i \overleftrightarrow{D}_\mu \varphi)(\bar{e}\gamma^\mu e)$	$O_{eu} = (\bar{e}\gamma_\mu e)(\bar{u}\gamma^\mu u)$
$O_{\phi q}^{(1)} = (\varphi^\dagger i \overleftrightarrow{D}_\mu \varphi)(\bar{q}\gamma^\mu q)$	$O_{ed} = (\bar{e}\gamma_\mu e)(\bar{d}\gamma^\mu d)$
$O_{\phi q}^{(3)} = (\varphi^\dagger i \overleftrightarrow{D}_\mu \tau^I \varphi)(\bar{q}\gamma^\mu\tau^I q)$	$O_{\ell u} = (\bar{\ell}\gamma_\mu\ell)(\bar{u}\gamma^\mu u)$
$O_{\phi u} = (\varphi^\dagger i \overleftrightarrow{D}_\mu \varphi)(\bar{u}\gamma^\mu u)$	$O_{\ell d} = (\bar{\ell}\gamma_\mu\ell)(\bar{d}\gamma^\mu d)$
$O_{\phi d} = (\varphi^\dagger i \overleftrightarrow{D}_\mu \varphi)(\bar{d}\gamma^\mu d)$	$O_{qe} = (\bar{q}\gamma_\mu q)(\bar{e}\gamma^\mu e)$

There is one more:

$$O_{\phi WB} = (\varphi^\dagger \tau^I \varphi) W_{\mu\nu}^I B^{\mu\nu} \Rightarrow \text{causes kinetic mixing of } W^3 \text{ and } B$$

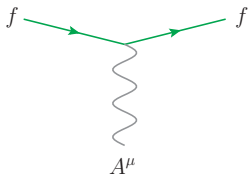
$$\Rightarrow \text{universally shifts the } ffV \text{ vertices after diagonalization that gives physical photon and Z boson states}$$

The ffV operators are already strongly bounded by Z and W pole observables (Dawson & Giardino [1909.02000]):

ffV	C_k	95% CL, $\Lambda = 1$ TeV
$O_{\phi\ell}^{(1)} = (\varphi^\dagger i \overleftrightarrow{D}_\mu \varphi) (\bar{\ell} \gamma^\mu \ell)$	$C_{\phi\ell}^{(1)}$	$[-0.043, 0.012]$
$O_{\phi\ell}^{(3)} = (\varphi^\dagger i \overleftrightarrow{D}_\mu \tau^I \varphi) (\bar{\ell} \gamma^\mu \tau^I \ell)$	$C_{\phi\ell}^{(3)}$	$[-0.012, 0.0029]$
$O_{\phi e} = (\varphi^\dagger i \overleftrightarrow{D}_\mu \varphi) (\bar{e} \gamma^\mu e)$	$C_{\phi e}$	$[-0.013, 0.0094]$
$O_{\phi q}^{(1)} = (\varphi^\dagger i \overleftrightarrow{D}_\mu \varphi) (\bar{q} \gamma^\mu q)$	$C_{\phi q}^{(1)}$	$[-0.027, 0.043]$
$O_{\phi q}^{(3)} = (\varphi^\dagger i \overleftrightarrow{D}_\mu \tau^I \varphi) (\bar{q} \gamma^\mu \tau^I q)$	$C_{\phi q}^{(3)}$	$[-0.011, 0.014]$
$O_{\phi u} = (\varphi^\dagger i \overleftrightarrow{D}_\mu \varphi) (\bar{u} \gamma^\mu u)$	$C_{\phi u}$	$[-0.072, 0.091]$
$O_{\phi d} = (\varphi^\dagger i \overleftrightarrow{D}_\mu \varphi) (\bar{d} \gamma^\mu d)$	$C_{\phi d}$	$[-0.16, 0.060]$
$O_{\phi WB} = (\varphi^\dagger \tau^I \varphi) W_{\mu\nu}^I B^{\mu\nu}$	$C_{\phi WB}$	$[-0.0088, 0.0013]$

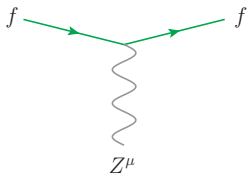
Thus, we restrict our attention only to the operators contributing to the $\ell\ell q q$ vertex, which leaves us with seven Wilson coefficients of interest: $C_{eu}, C_{ed}, C_{\ell q}^{(1)}, C_{\ell q}^{(3)}, C_{lu}, C_{ld},$ and C_{qe} .

Since we consider contributions only to the $\ell\ell qq$ interaction, we assume the usual SM ffV vertices in our analysis:



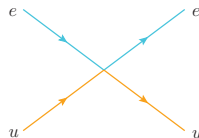
$$g_1^{(fA)} = -eQ_f$$

$$g_5^{(fA)} = 0$$



$$g_1^{(fZ)} = g_V^f$$

$$g_5^{(fZ)} = g_A^f$$

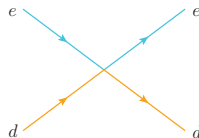


$$g_{11}^{(eu)} = \frac{1}{4} [C_{eu} + (C_{\ell q}^{(1)} - C_{\ell q}^{(3)}) + C_{\ell u} + C_{qe}]$$

$$g_{15}^{(eu)} = \frac{1}{4} [C_{eu} - (C_{\ell q}^{(1)} - C_{\ell q}^{(3)}) + C_{\ell u} - C_{qe}]$$

$$g_{51}^{(eu)} = \frac{1}{4} [C_{eu} - (C_{\ell q}^{(1)} - C_{\ell q}^{(3)}) - C_{\ell u} + C_{qe}]$$

$$g_{55}^{(eu)} = \frac{1}{4} [C_{eu} + (C_{\ell q}^{(1)} - C_{\ell q}^{(3)}) - C_{\ell u} - C_{qe}]$$



the same as for $eeuu$ but with $u \rightarrow d$ and

$$C_{\ell q}^{(1)} - C_{\ell q}^{(3)} \rightarrow C_{\ell q}^{(1)} + C_{\ell q}^{(3)}$$

Amplitude and cross section for $\ell + q \rightarrow \ell' + q'$:

$$\mathcal{M} = \mathcal{M}_\gamma + \mathcal{M}_Z + \mathcal{M}_\times \Rightarrow d\sigma^{\lambda_\ell \lambda_q} = \frac{d^2\sigma}{dx dQ^2} = \frac{1}{16\pi x^2 s^2} |\mathcal{M}|^2 + \mathcal{O}(C_k^2)$$

Asymmetry definitions:

- unpolarized PV asymmetries: $A_{PV} = \frac{d\sigma_\ell}{d\sigma_0}$
- polarized PV asymmetries: $\Delta A_{PV} = \frac{d\sigma_H}{d\sigma_0}$
- lepton-charge asymmetries: $A_{LC} = \frac{d\sigma_0(e^+H) - d\sigma_0(e^-H)}{d\sigma_0(e^+H) + d\sigma_0(e^-H)}$

where

$$d\sigma_0 = \frac{1}{4} \sum_q f_{q/H} [d\sigma^{++} + d\sigma^{+-} + d\sigma^{-+} + d\sigma^{--}] : \text{unpol. } \ell + \text{unpol. } H$$

$$d\sigma_\ell = \frac{1}{4} \sum_q f_{q/H} [d\sigma^{++} + d\sigma^{+-} - d\sigma^{-+} - d\sigma^{--}] : \text{pol. } \ell + \text{unpol. } H$$

$$d\sigma_H = \frac{1}{4} \sum_q \Delta f_{q/H} [d\sigma^{++} - d\sigma^{+-} + d\sigma^{-+} - d\sigma^{--}] : \text{unpol. } \ell + \text{pol. } H$$

Data sets, shown with beam energies and nominal annual luminosities:

D1	5 GeV × 41 GeV eD , 4.4 fb ⁻¹
D2	5 GeV × 100 GeV eD , 36.8 fb ⁻¹
D3	10 GeV × 100 GeV eD , 44.8 fb ⁻¹
D4	10 GeV × 137 GeV eD , 100 fb ⁻¹
D5	18 GeV × 137 GeV eD , 15.4 fb ⁻¹
P1	5 GeV × 41 GeV ep , 4.4 fb ⁻¹
P2	5 GeV × 100 GeV ep , 36.8 fb ⁻¹
P3	10 GeV × 100 GeV ep , 44.8 fb ⁻¹
P4	10 GeV × 275 GeV ep , 100 fb ⁻¹
P5	18 GeV × 275 GeV ep , 15.4 fb ⁻¹
P6	18 GeV × 275 GeV ep , 100 fb ⁻¹

P6: Yellow Report reference setting [2103.05419]

Data set labels:

D, P: unpolarized PV asymmetry

ΔD, ΔP: polarized PV asymmetry

LD, LP: lepton-charge asymmetry

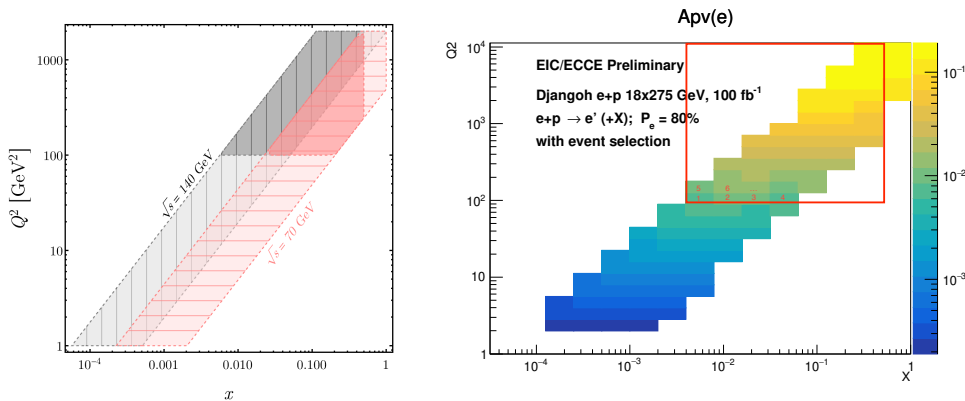
Cuts on projected data:

$Q > 1 \text{ GeV}$	to avoid nonperturbative QCD
$y > 0.1$	to avoid bin migration and unfolding uncertainty
$y < 0.9$	to avoid high photoproduction background due to final-state hadron
$ \eta < 3.5$	to restrict events in main acceptance of ECCE detector
$E' > 2 \text{ GeV}$	to have high-purity e^- samples

Additional cuts in SMEFT analysis:

$x < 0.5$	to avoid <i>large</i> uncertainties from nonperturbative QCD and nuclear dynamics
$Q > 10 \text{ GeV}$	

Kinematic region of the data sets ($\sqrt{s} = 70\text{-}140$ GeV, $0.1 \leq y \leq 0.9$):

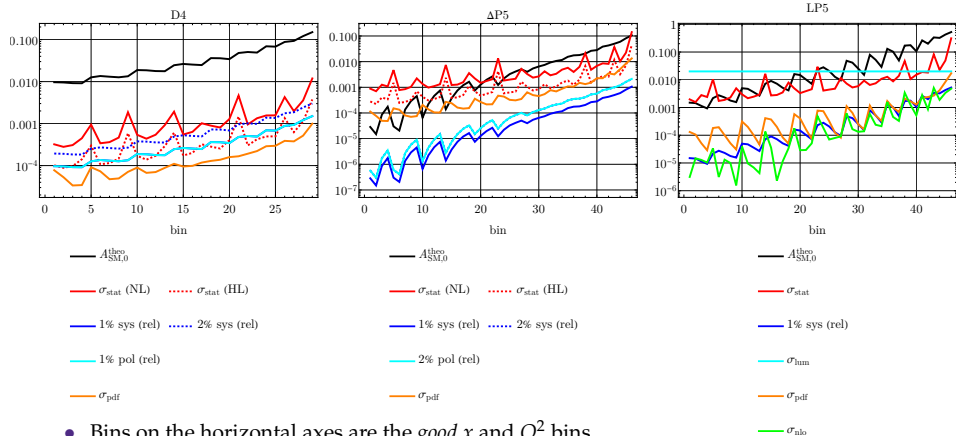


The shaded region on the left and the red box on the right indicate the kinematic region and *good* bins used in our SMEFT analysis, respectively.

Anticipated uncertainty components:

Error type	$A_{PV}(D, P)$	$\Delta A_{PV}(\Delta D, \Delta P)$	$A_{LC}(LD, LP)$
statistical (NL)	$\sigma_{\text{stat}} = \frac{1}{P_\ell \sqrt{N}}$	$\frac{P_\ell}{P_H} \sigma_{\text{stat}}$	$\sqrt{10} P_\ell \sigma_{\text{stat}}$
statistical (HL)	$\frac{1}{\sqrt{10}} \sigma_{\text{stat}}$	$\frac{1}{\sqrt{10}} \frac{P_\ell}{P_H} \sigma_{\text{stat}}$	✗
uncorrelated systematic	1% rel.	1% rel.	1% rel.
fully correlated beam polarization	1% rel.	2% rel.	✗
fully correlated luminosity	✗	✗	2% abs.
uncorrelated QED NLO	✗	✗	$5\% \times (A_{LC}^{\text{NLO}} - A_{LC}^{\text{Born}})$
fully correlated PDF	✓	✓	✓

PDF sets used: NNPDF3.1 NLO and NNPDFpo11.1



- Bins on the horizontal axes are the *good* x and Q^2 bins.
- Stat error dominates in PV asymmetries in NL case.
- Systematic and **beam-polarization** errors become comparable to stat error in HL case.
- **Luminosity** error dominates in LC asymmetries.
- Stat error competes with **luminosity** error at high- x high- Q^2 bins.
- PDF errors are the least dominant in **unpolarized** PV asymmetries but become significant in the **polarized** case.

Pseudodata generation:

$$A_{\text{pseudo},b}^{(e)} = A_{\text{SM},b} + r_b^{(e)} \sigma_b^{\text{unc}} + r_b^{\prime(e)} \sigma_b^{\text{cor}}$$

$$b \in \text{Range}(N_{\text{bin}}), \quad e \in \text{Range}(N_{\text{exp}}), \quad N_{\text{exp}} = 10^3, \quad r_b^{(e)}, r_b^{\prime(e)} \sim \mathcal{N}(0, 1)$$

$$\sigma_b^{\text{unc}} = \sigma_{\text{stat},b} \oplus \sigma_{\text{sys},b}$$

$$\sigma_b^{\text{unc}} = \sigma_{\text{stat},b} \oplus \sigma_{\text{sys},b} \oplus \sigma_{\text{nlo},b}$$

$$\sigma_b^{\text{cor}} = \sigma_{\text{pol},b}$$

$$\sigma_b^{\text{cor}} = \sigma_{\text{lum},b}$$

SMEFT asymmetry expressions:

$$A_{\text{SMEFT},b} = A_{\text{SM},b} + \sum_{k=1}^{N_{\text{fit}}} C_k \delta A_{k,b} + \mathcal{O}(C_k^2), \quad N_{\text{fit}} \in \text{Range}(7)$$

χ^2 function for each pseudoexperiment:

$$\chi^2^{(e)} = \sum_{b,b'=1}^{N_{\text{bin}}} [A_{\text{SMEFT},b} - A_{\text{pseudo},b}^{(e)}] H_{bb'} [A_{\text{SMEFT},b'} - A_{\text{pseudo},b'}^{(e)}]$$

Polarimetry and **luminosity difference** can be limiting factors.

- ⇒ use data itself to constrain these systematic effects
- ⇒ simultaneous fits of C_k with **beam polarization**, P , and **luminosity difference**, A_{lum} , in an attempt to obtain stronger bounds for C_k

Fits of C_k with P :

$$\chi^2(e) = \sum_{b,b'=1}^{N_{\text{bin}}} [PA_{\text{SMEFT},b} - A_{\text{pseudo},b}^{(e)}] \left[H_{bb'} \Big|_{\sigma_{\text{pol}} \rightarrow 0} \right] [PA_{\text{SMEFT},b'} - A_{\text{pseudo},b'}^{(e)}] + \frac{(P - \bar{P})^2}{\delta P^2}$$

unpolarized PV asymmetries:

- $|\rho(C_k, P)| \gtrsim 0.7$
- **30-50% stronger bounds**

polarized PV asymmetries:

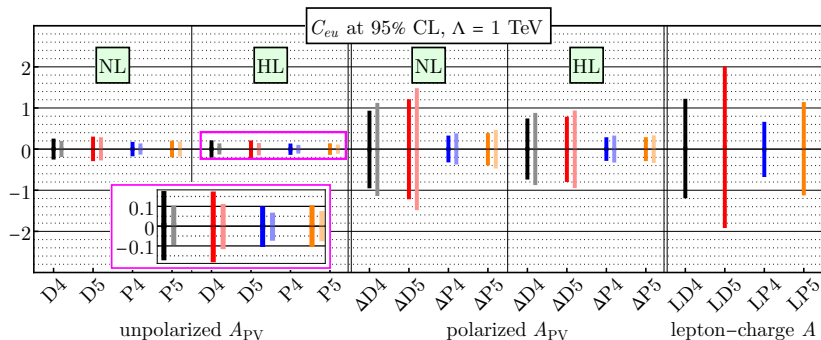
- $|\rho(C_k, P)| \lesssim 0.2$
- **15-20% weaker bounds**

Improvement is more significant than worsening ⇒ include P in fits.

Fits of C_k with A_{lum} :

$$\chi^2(e) = \sum_{b,b'=1}^{N_{\text{bin}}} [A_{\text{SMEFT},b} - A_{\text{pseudo},b}^{(e)} - A_{\text{lum}}] \left[H_{bb'} \Big|_{\sigma_{\text{lum}} \rightarrow 0} \right] [A_{\text{SMEFT},b'} - A_{\text{pseudo},b'}^{(e)} - A_{\text{lum}}]$$

Mild correlations, $|\rho(C_k, A_{\text{lum}})| \lesssim 0.4$, leading to **15-20% weaker bounds**
 ⇒ do not include A_{lum} in fits.

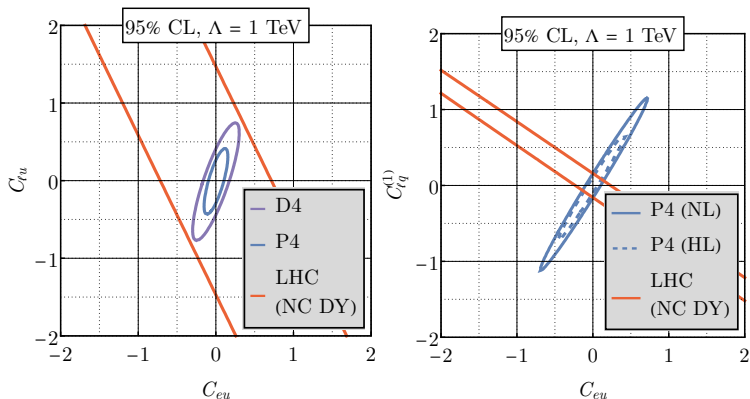


In terms of the strength of bounds:

- proton > deuteron
- high-lum. low-energy (4th sets) > low-lum. high-energy (5th sets)
- unpolarized PV > polarized PV > lepton-charge
- improvement: unpolarized PV > polarized PV if NL \rightarrow HL

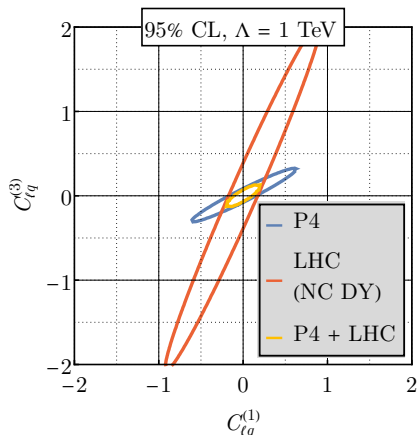
Corresponding effective UV scales: 3 TeV with NL, 4 TeV with HL

Compare the bounds from deuteron and proton data of **unpolarized** PV asymmetries to the 8-TeV 20-fb⁻¹ LHC NC DY data (Boughezal, Petriello, & Wiegand [2004.00748, 2104.03979]):



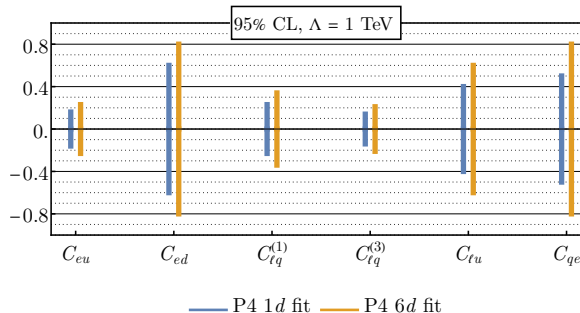
Distinct correlations: EIC fits are complementary to LHC NC DY. However, LHC fits have **blind spots** and exhibit **flat directions**, which remain **even in the high-luminosity case**. The EIC can resolve and constrain this parameter space strongly.

Compare proton data of **unpolarized** PV asymmetries to the 8-TeV 20-fb⁻¹ LHC NC DY data (Boughezal, Petriello, & Wiegand [2004.00748]) when the LHC fit doesn't have a flat direction:



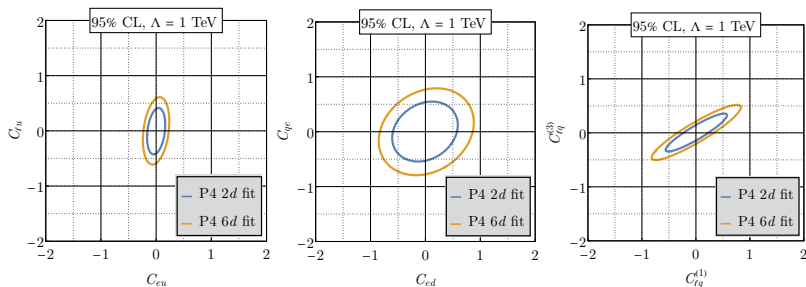
Distinct correlations again: EIC fits are complementary to LHC NC DY. Moreover, when the LHC fit gives a strong bound without showing a flat direction, the EIC can constrain the same parameter space even more strongly.

N_{fit}	N_{exp}
2	10^3
3	10^4
4	10^5
5	10^6
6	10^7
7	10^8 (?!)



- Number of pseudoexperiments increases to reflect the required statistics.
- **Beam polarization** parameter, P , is not included here.
- Bounds become 25 to 40% weaker due to increased number of fitted parameters and correlations among them.
- Not significant worsening because correlations dominate statistical effect of increasing number of fitted parameters.

Compare the two-parameter fits of Wilson coefficients to the projections from a six-parameter fit:



- The $eeuu$ vertex contains the combination $C_{lq}^{(1)} - C_{lq}^{(3)}$ and the $eedd$ vertex has $C_{lq}^{(1)} + C_{lq}^{(3)}$.
- These may lead to degeneracies and flat directions in a multi-parameter fit of Wilson coefficients.
- The EIC can resolve this part of the parameter space, imposing strong bounds.

- We investigate the BSM potential of EIC in the model-independent SMEFT framework by focusing on semi-leptonic four-fermion operators at dimension 6 by giving a detailed accounting of uncertainties.
- We obtain bounds on Wilson coefficients from single-, double-, and even multiple-parameter fits by using techniques to simultaneously fit P and A_{lum} together with SMEFT parameters.

- We find that UV scales up to 3 TeV (or 4 TeV) can be probed with nominal (or $10\times$ high) annual luminosity.
- We observe that the strongest bounds come from **unpolarized** PV asymmetries of proton.
- EIC is shown to be complementary and competitive to LHC NC DY by
 - equally or more strongly confining the Wilson coefficients with distinct correlations;
 - resolving the degeneracies observed in the LHC data.

EIC was designed as a QCD machine and it shows strong potential for BSM physics.